WOODY COVER ASSESSMENTS IN A SOUTHERN AFRICAN SAVANNA, USING HYPER-TEMPORAL C-BAND ASAR-WS DATA

Russell Main [1], Renaud Mathieu [1], Waldo Kleynhans [2], Konrad Wessels [2], Laven Naidoo [1], Gregory P. Asner [3]

[1] Ecosystems Earth Observation, Natural Resources and the Environment, CSIR, Pretoria, South Africa
[2] Remote Sensing Research Unit, Meraka Institute, CSIR, Pretoria, South Africa
[3] Department of Global Ecology, Carnegie Institution for Science, Stanford, CA, USA

ABSTRACT

Southern African savanna ecosystems and their woody resources are under pressure. Governments in the region need locally calibrated, cost effective, and regularly updated information on these resources in order to satisfy both national and international commitments to manage them. Using LiDAR data as a calibration dataset, this paper sets out to investigate the potential of hyper-temporal C-band ASAR SAR data in mapping woody structural related parameters in a savanna environment. Images spanning three years where grouped by years (2007-2009), season (Wet or Dry) and polarization (HH or VV), and relationships were sought for the woody parameter total canopy cover (TCC). Results show that: Dry season combinations of images outperformed wet season images; HH co-polarised images outperformed VV images; temporally filtered images showed marked improvement on unfiltered images. While non-parametric random forest models achieved better validation accuracies than other models did. The single best result was achieved by combining all the temporally filtered images, from all of the various scenarios (R^2=0.74; RMSE=8.52; SEP=35.27). The results show promise in delivering regional scale, locally calibrated, baseline products for the management of Southern Africa's woody resources.

Index Terms— Cover, Savanna, ASAR, Hyper-temporal, C-Band

1. INTRODUCTION

Savanna ecosystems are ecologically and economically significant systems that are defined by a continuous herbaceous layer interspersed with trees [1], [2]. They cover more than 30% of the worlds vegetated land surface, and more than half of the African continent, thereby providing millions of mostly poorer households with the materials they need in order to buffer the full effects of poverty[2]. Woody resources hold great carbon sequestration potential, but are facing over-utilisation in some regions, while in others their encroachment threatens the availability of viable grazing land. The (potential) impacts of these combined pressures on woody resources in the Southern African region need to be monitored in order to avoid significant losses, both in terms of associated ecosystem services, and the livelihoods dependant them. This requires being able to accurately measure, report, and verify available woody resources in order that they are sustainably managed.

To date, the most up-to-date information of this kind are in the form of global products, which are poorly calibrated outside of boreal and tropical forest environments and show poor accuracies for regions such as Southern Africa.

Space-borne synthetic aperture radar (SAR) sensors have had success in measuring and mapping woody vegetation over large areas of interest, largely due to the canopy penetration capabilities of the SAR signal, as well as its ability to capture data despite the presence of cloud cover. C-band SAR has proven capable of reliably estimating certain forest parameters (in tropical and boreal forests) when multi-date data are used. The inclusion of temporal data is theorised to increase the contribution of the SAR signal from vegetation while reduce or smooth the signal from other backscatter sources [3]. Recent studies have provided promising results (i.e. R^2=0.69-0.75) when using repeat pass C-band imagery to relate backscatter to savanna woody structural parameters (i.e. canopy volume, and cover) [4].

Whereas the aforementioned studies used small footprint, high resolution, commercial C-band sensors (e.g. RADARSAT2), there remains a need in savanna woodlands to establish the estimation protocols necessary for more regional scale assessments using affordable coarse resolution sensors. The (decommissioned) ENVISAT ASAR archive data holds the potential of delivering locally calibrated baseline (woody structure) products to government agencies that have only ever had access to global models (i.e. MODIS VCF). These baseline products can then act as points of departure for exploiting data produced by the new ESA SAR C-band sensor (Sentinel-1) launched early 2014.

Using the hyper-temporal ASAR C-band data, the objectives of the study were to explore specific scenarios under which the SAR data had the strongest relationships with woody cover in a savanna environment. Scenarios tested comprised of images that were a) temporally filtered or unfiltered, b) single year or multi-year combinations, c) split into wet, dry or multi-season, and/or d) split into co-polarised HH, VV or a combination of both

2. STUDY AREA AND METHODS

The study area is situated in the Lowveld region of the savanna biome at the north-eastern edge of South Africa. Rainfall primarily

occurs in the summer months between October and May. The range of woody canopy cover can be from 5% in the open savanna, to 60% in woodland areas, and 80% in riparian areas [5].

Airborne LiDAR data was used to calibrate and validate predictive SAR models for total woody cover. The LiDAR data totalled approximately 35 000 ha, and was flown over various sites within the study area during April-May 2008 using the Carnegie Airborne Observatory (CAO) Alpha system [6]. Total canopy cover (TCC) was calculated as the percentage area that is occupied by woody vegetation (woody plants > 0.5m in height).

The hyper-temporal SAR data consisted of 55 irregularly timed Envisat ASAR wide-swath mode images (~70x76m resolution) acquired between January 2007 and December 2009. Given the scarcity of multi-year LiDAR acquisitions, it was assumed that there was little significant change in the total woody cover of the area from when the LiDAR was acquired (i.e. 2008), and therefore SAR data from the preceding (i.e. 2007) and subsequent (i.e. 2009) years could be used to build a hyper-temporal dataset and relate it to the LiDAR. The 55 images consisted of 22 wet (November to April) and 33 dry (May to October) season images, as well as both available polarisations, namely HH (44 images) and VV (11 images). Each image was radiometrically and geometrically pre-processed using GAMMA software, masked to the study area, and resampled to 75m x 75m. All the chosen images had 100% coverage of the region of interest.

We considered a number of different modelling scenarios, which included single or multi-year combinations (2007, 2008, 2009), different seasons (wet (W), dry (D) or both), and polarisations (HH, VV, or both). Images of different polarisations or seasons were not mixed; so it was only in the modelling of these different scenarios that the seasons or polarisations were combined (i.e. scenarios "HHVV" or "WD").We also considered scenarios where the images were either unfiltered or were temporally filtered, after [7]. The temporal filter sets out to linearly combine images of a given time series, in order to create a new set of speckle reduced images. The filter uses the input intensity data, as well as a local mean backscattering coefficient that is estimated in a window around each pixel[7]. The filter serves to reduce the variance (i.e. speckle) within the image, while preserving both radiometric and spatial resolution. Temporal filtering of image stacks can be negatively influenced by sporadic and episodic rainfall or fire events. Heavy rainfall events would increase the soil moisture effects on the SAR signal, and result in artificially high values, while fire events would remove significant amounts of vegetation. By colour compositing images from different dates, we visually assessed the images for obvious signs of these events and removed the necessary images from both the unfiltered and filtered analyses. Three different filter windows sizes were tested, namely 3x3, 7x7, and 11x11 pixels

The sampling approach followed the "block" spatial aggregation method [4], whereby a grid of 150m polygons, spaced 75m apart, were used to extract data from each of the LiDAR and SAR datasets. After splitting the sample dataset (n=3852) into 35% training and 65% test, the multi-linear and random forest regression models were used to predict TCC using the different SAR scenarios.

3. RESULTS & DISCUSSION

In Table 1 a subset of the accuracies for the different SAR scenarios in predicting the LiDAR metric (TCC) are presented, and ranked by increasing RMSE. Only the multi-year scenarios are presented here, as no single year scenario outperformed its multi-year equivalent. The non-parametric random forest model (ntrees=500, mtry=sqrt[no. variables]) produced only slightly better accuracies than the linear model throughout the study. There are bigger differences between the different image scenarios than there are between the different models. The improved performance of the random forest method is to be expected as the SAR and LiDAR metric relationship is slightly non-linear, and likely to saturate towards the top end of the range.

Table 1: Modelling results for TCC under different filtering treatments, and image scenarios. The scenarios are defined by year (2007-2009), polarisation (HH or VV), or season (W or D).

	TCC						
	Linear Regression			Random Forest			
Scenario	R^2	RMSE	SEP	R^2	RMSE	SEP	Variables
Unfiltered							
2007to2009_HHVV_WD	0.64	9.94	41.16	**0.65**	**9.86**	**40.85**	55
2007to2009_HHVV_D	0.60	10.49	43.19	0.62	10.14	41.75	33
2007to2009_HH_WD	0.61	10.29	42.65	0.62	10.25	42.47	44
2007to2009_HH_D	0.58	10.75	44.40	0.60	10.57	43.67	26
2007to2009_VV_WD	0.50	11.72	49.28	0.58	10.62	44.64	11
2007to2009_VV_D	0.49	11.98	49.62	0.56	10.95	45.35	7
2007to2009_HHVV_W	0.49	11.78	48.66	0.51	11.57	47.79	22
2007to2009_HH_W	0.44	12.32	50.63	0.45	12.27	50.42	18
2007to2009_VV_W	0.24	14.70	60.07	0.32	13.61	55.60	4
Temporal Filter (11x11)							
2007to2009_HHVV_WD	0.72	8.70	36.00	**0.74**	**8.52**	**35.27**	55
2007to2009_HH_WD	0.70	9.11	38.09	0.72	8.80	36.81	44
2007to2009_HHVV_D	0.68	9.44	38.82	0.70	9.15	37.62	33
2007to2009_HH_D	0.66	9.60	39.56	0.68	9.31	38.39	26
2007to2009_VV_WD	0.65	9.81	40.83	0.67	9.48	39.43	11
2007to2009_VV_D	0.62	10.20	41.76	0.65	9.74	39.88	7
2007to2009_HHVV_W	0.59	10.61	44.31	0.64	10.00	41.74	22
2007to2009_HH_W	0.55	11.06	45.57	0.63	10.05	41.38	18
2007to2009_VV_W	0.42	12.60	53.01	0.44	12.30	51.75	4

*R^2 = coefficient of determination; SEP = Standard error of prediction (%); RMSE = Root mean square error (%)

For both the unfiltered and filtered treatments, the scenario that included the images from all three years, both polarisations (HH and VV), and both seasons (W and D) produced the best results (i.e. 2007to2009_HHVV_WD). Dry season scenarios, for all three combinations of polarisation (i.e. HHVV/HH/VV) consistently outperformed Wet season scenarios. Similarly, HH scenarios, for all three combinations of seasons (i.e. WD/D/W) generally outperformed the equivalent VV scenarios. The performance of the dry season images over the wet season images is consistent with other literature, which indicates dry, conditions to be the best for vegetation parameter estimation using SAR [3], [4]. This is partly due an increased transparency within the canopy that allows the SAR signal to penetrate further into the canopy and interact with the larger elements of the tree, as well as a decrease in the

influence of soil or grass moisture contents [3]. "Leaf-off" conditions result in surface and single bounce scattering to be more prominent than in "leaf-on" conditions [4]. Co-polarised images (HH and VV) are more representative of surface scattering elements, as opposed to cross-polarised images (i.e. HV) being more representative of volume scattering, and are therefore able to produce the strong relationships as seen in Table 1..

The temporal filter acted to reduce the amount of variance (i.e. speckle) in the images, and in doing so improved upon the unfiltered prediction accuracies for TCC, in every scenario. Of the three filter window sizes tested (3x3, 7x7, and 11x11); only the best performing 11x11 window results are presented in Table 1. The performance of the filter is also evidenced in the increase of the equivalent number of looks (ENL) for the SAR images, which was ~11.5 for the unfiltered images, and became ~40 for the filtered images. The ENL is defined as the ratio between the squared mean and the variance of the intensity, and is often used to gauge the performance of speckle filters.
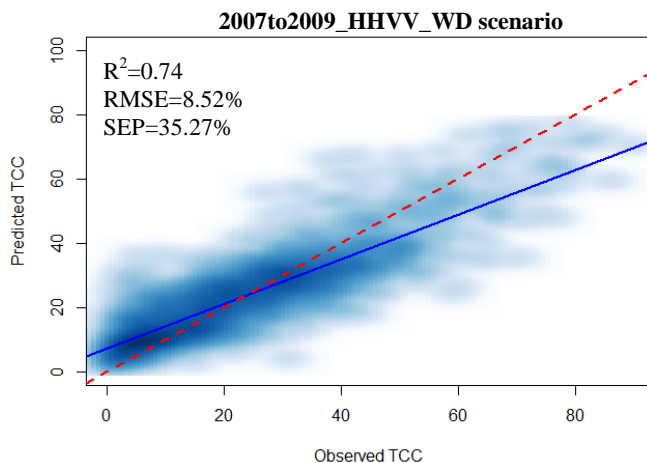
Figure 1: Observed versus predicted scatter plots for TCC, using temporally filtered images.

The observed versus predicted scatter plots are presented in Fig. 2, for the best performing filtered image scenario (*2007to2009_HHVV_WD*). In comparison to the 1:1 line, it is clear that the TCC model is overestimating values at the lower end of the range, and underestimating values at the top end of the range.

The underestimation in high cover areas can be explained by the C-band signals limited ability in penetrating a dense canopy [8]. The LiDAR coverage also had a limited amount of very dense vegetation which could be sampled; hence the top end of the TCC range is under-represented. At the lower end, limitations of the LiDAR in detecting very small vegetation would contribute to the overestimation [9], as would the interference and variability of soil textures and grass biomass in these low woody cover areas.

In summary, the filtered multi-year combinations of images produced a marked improvement over unfiltered single year images. While there was also a clear improvement in making use of dry season images over wet season images, although the combination of the two seasons outperformed the equivalent scenario using one season (i.e. HH_WD outperformed HH_D). HH over VV scenarios show improvements to a lesser degree than the improvements shown between seasons, but again the combination of HH and VV images produced better results than the equivalent

scenario using only one polarisation (i.e. HHVV_D outperformed HH_D). From an operational point of view, in terms of producing regional scale products, the HH wet and dry season images produce good results and it may be worth weighing up a small gain in accuracy versus the time necessary to process the additional VV images.

4. CONCLUSIONS

We investigated the effectiveness of course scale, C-band, hyper-temporal ASAR-WS imagery in extracting total canopy cover metrics in a Southern African savanna environment. The temporally filtered scenario that consisted of all the images, from each of the polarisations and seasons, produced the single best result (i.e. R^2=0.74; RMSE=8.52). The results of the paper are encouraging, when considered in the context that neither the SAR wavelength (i.e. C-band), the spatial resolution (i.e.75m), nor the single polarisation (i.e. HH and VV) are known to be optimal SAR parameters for vegetation mapping, especially in an environment with high levels of spatial heterogeneity. This is where the hyper-temporal dataset has contributed to off-set these disadvantages and produce results that show potential for regional scale mapping of woody parameters, which could form the baseline products from which future monitoring programmes will compare. The study is unique in its application of the methods to the above mentioned dataset in a woody savanna environment. The process of collecting additional LiDAR calibration data is under way in order to strengthen the models and investigate their performance in areas of higher cover, and that may be experiencing higher degrees of change (i.e. commercial forestry regions) Investigations are also under way to expand the current study to include further analysis on the performance of temporal filters in these environments, as well as to include additional LiDAR metrics such as total canopy volume (TCV) as an additional variable.

5. ACKNOWLEDGEMENTS

5. REFERENCES

[1]   M. Sankaran, N. P. Hanan, R. J. Scholes, et al., "Determinants of woody cover in African savannas.," *Nature*, vol. 438, no. 7069, pp. 846–9, Dec. 2005.

[2]   R. J. Scholes and S. Archer, "Tree-grass interactions in savannas," *Annu. Rev. Ecol. Syst.*, vol. 28, pp. 517–544, 1997.

[3]   M. Santoro, C. Beer, O. Cartus, et al., "Retrieval of growing stock volume in boreal forest using hyper-temporal series of Envisat ASAR ScanSAR backscatter measurements," *Remote Sens. Environ.*, vol. 115, no. 2, pp. 490–507, Feb. 2011.

[4]   R. Mathieu, L. Naidoo, M. a. Cho, et al., "Toward structural assessment of semi-arid African savannahs and woodlands: The potential of multitemporal polarimetric RADARSAT-2 fine beam images," *Remote Sens. Environ.*, vol. 138, pp. 215–231, Nov. 2013.

[5]   K. J. Venter, R. J. Scholes, and H. C. Eckhardt, "The abiotic template and its associated vegetation pattern," in *The Kruger experience: Ecology and management of savanna heterogeneity*, vol. 21, no. 1, J. du Toit, K. Rogers, and H. Biggs, Eds. London: Island Press, 2003, pp. 83–129.

[6]   G. P. Asner, D. E. Knapp, T. Kennedy-Bowdoin, et al., "Carnegie Airborne Observatory: in-flight fusion of hyperspectral imaging and waveform light detection and ranging for three-dimensional studies of ecosystems," *J. Appl. Remote Sens.*, vol. 1, no. 1, pp. 1–21, Sep. 2007.

[7]   S. Quegan and J. J. Yu, "Filtering of Multichannel SAR Images," *IEEE Trans. Geosci. Remote Sens.*, vol. 39, no. 11, pp. 2373–2379, 2001.

[8]   M. C. Dobson, F. T. Ulaby, T. Le Toan, et al., "Dependence of radar backscatter on coniferous forest biomass.," *IEEE Trans. Geosci. Remote Sens.*, vol. 30, no. 2, pp. 412–415, 1992.

[9]   K. J. Wessels, R. Mathieu, B. F. N. Erasmus, et al., "Impact of communal land use and conservation on woody vegetation structure in the Lowveld savannas of South Africa," *For. Ecol. Manage.*, vol. 261, no. 1, pp. 19–29, Jan. 2011.